Report

Current Biology

Active Control of Cell Size Generates Spatial Detail during Plant Organogenesis

Graphical Abstract

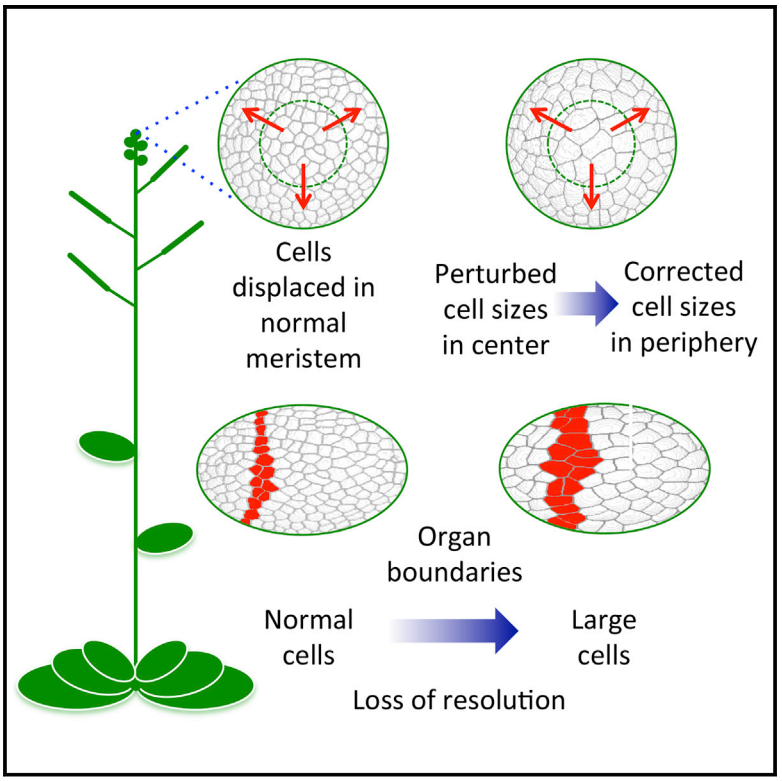

Authors

Antonio Serrano-Mislata, Katharina Schiessl, Robert Sablowski

Correspondence

robert.sablowski@jic.ac.uk

In Brief

Different cell types have characteristic sizes, but it unclear how cell size is maintained and why it matters. Serrano-Mislata et al. show that plant meristem cells actively maintain a target size, which is required to generate fine detail during development, similar to the way appropriate pixel sizes are needed to render detail in digital images

Highlights

- Cell divisions are unequal and cell growth is heterogeneous in the meristem
- Simulations indicate that growth and cell cycle are coordinated in individual cells
- Meristem cell sizes are rapidly corrected after perturbation
- Abnormal cell sizes do not affect growth but perturb organ boundaries and emergence

Serrano-Mislata et al., 2015, Current Biology *25*, 2991–2996
November 16, 2015
http://dx.doi.org/10.1016/j.cub.2015.10.008

CellPress

Current Biology
Report

Active Control of Cell Size Generates Spatial Detail during Plant Organogenesis

Antonio Serrano-Mislata,[1] Katharina Schiessl,[1] and Robert Sablowski[1,*]
[1]Cell and Developmental Biology Department, John Innes Centre, Norwich Research Park, Norwich NR4 7UH, UK
*Correspondence: robert.sablowski@jic.ac.uk
http://dx.doi.org/10.1016/j.cub.2015.10.008

SUMMARY

How cells regulate their dimensions is a long-standing question [1, 2]. In fission and budding yeast, cell-cycle progression depends on cell size, although it is still unclear how size is assessed [3–5]. In animals, it has been suggested that cell size is modulated primarily by the balance of external signals controlling growth and the cell cycle [1], although there is evidence of cell-autonomous control in cell cultures [6–9]. Regardless of whether regulation is external or cell autonomous, the role of cell-size control in the development of multicellular organisms remains unclear. Plants are a convenient system to study this question: the shoot meristem, which continuously provides new cells to form new organs, maintains a population of actively dividing and characteristically small cells for extended periods [10]. Here, we used live imaging and quantitative, 4D image analysis to measure the sources of cell-size variability in the meristem and then used these measurements in computer simulations to show that the uniform cell sizes seen in the meristem likely require coordinated control of cell growth and cell cycle in individual cells. A genetically induced transient increase in cell size was quickly corrected by more frequent cell division, showing that the cell cycle was adjusted to maintain cell-size homeostasis. Genetically altered cell sizes had little effect on tissue growth but perturbed the establishment of organ boundaries and the emergence of organ primordia. We conclude that meristem cells actively control their sizes to achieve the resolution required to pattern small-scale structures.

RESULTS

Unequal Cell Divisions and Heterogeneous Cell Growth Introduce Cell-Size Variability in the Meristem

The absence of cell migration and the relatively easy access to the shoot apical meristem facilitate the analysis of how cell growth and division are coordinated during multicellular development. To track cell growth and division, we used time-lapse confocal imaging of excised *Arabidopsis* inflorescence apices [11, 12] and developed a package of Python scripts and Fiji macros to landmark, segment, locate, track, and measure cells in 3D (3D_meristem_analysis, source code, and detailed description in Supplemental Information) (Figures 1A and 1B). Images were manually curated to delete cells that were incorrectly segmented or tracked; all experiments focused on cells in the two outer meristem layers (L1, L2), for which segmentation accuracy was higher. Using independent images of the same apex at two different angles, the average coefficient of variation for the volumes of matched cells was 5.4% (three apices, n = 1,902) (Figure S1).

Coordination between cell growth and cell cycle not only sets the average cell size, but also constrains its variability [2]. To assess whether the uniformity of meristem cells is consistent with active control of cell sizes, we first measured the sources of size variability. Meristem cell divisions were often unequal (Figures 1D and 1F). Division ratios (defined as the volume of each sibling cell relative to their combined volume) varied between 23% and 77%, with a SD of 9.4%–11.8% (95% confidence interval, Table S1), comparable to the 9.3% reported using cell areas [14]. The coefficient of variation (CV) of mother cell volumes was significantly lower than for their daughter cells, confirming that unequal divisions increased cell-size variability during a single cell generation (Figure 1G).

A key question in cell-size homeostasis is how growth rate relates to cell volume: the initial variability caused by unequal divisions could be either amplified by exponential growth (i.e., if cells have the same relative growth rate regardless of size) or reduced, if larger cells grew relatively less [15]. Furthermore, feedback between mechanical stress and local growth rates, which causes heterogeneity in the growth of neighboring cells [16], could potentially couple growth rates to cell sizes. In the meristem, relative growth rates showed a weak but significant negative correlation with cell volumes ($r = -0.17$, $p = 8.74\text{e-}13$) (Figure 1H), rejecting the hypothesis of exponential growth, but at the same time indicating that most of the variation in growth rate was not related to cell volume. Similar results were obtained using only cells in the central region of the meristem (Table S1), suggesting that this variability is not due to regional differences in meristem growth. Visual inspection confirmed that neighboring meristem cells with similar volume often had divergent growth rates (Figures 1C–1F). In conclusion, rather than causing cell sizes to converge, local growth heterogeneity could add to the variability introduced by unequal cell divisions, while the negative correlation between growth rate and cell volume, albeit weak, might still constrain cell-size variability in the meristem.

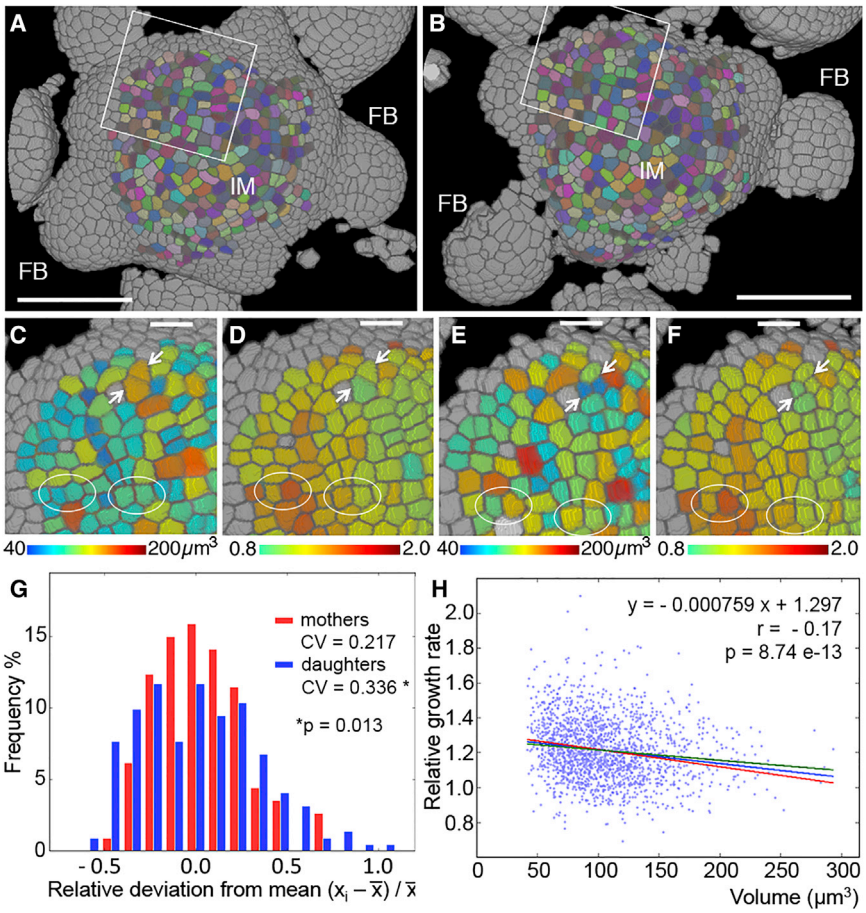

Figure 1. Sources of Cell-Size Variability in the Shoot Meristem

(A and B) Segmented images of wild-type inflorescence apices at 0 (A) and 24 hr later (B), with matching cells in the same color; regions in white rectangles in (A) and (B) correspond to (C)–(F); IM, inflorescence meristem; FB, floral bud.

(C–F) Close-up view of regions highlighted in (A) (C and D) and (B) (E and F), with cells labeled by volume (C and E) or relative growth rate over 24 hr (D and F); arrows show unequal divisions and encircled pairs of cells had similar volumes at 0 hr but different growth rates.

(G) Deviation from the mean volume for cells that divided over 24 hr (red bars) and their daughter cells (blue bars); the p value is for equality of coefficients of variation (Levene's test on relative deviations from mean) [13].

(H) Scatterplot of relative growth rates over 24 hr as a function of cell volume and corresponding linear regression (blue line), with regression function and r and p values (Pearson correlation) indicated; green and red lines show the limits of the 95% confidence interval for the slope.

Scale bars, 50 (A and B) 10 μm (C–F). See also Figure S1.

Maintenance of Uniform Sizes Is Likely to Require Coordination of Cell Growth and Cell Cycle in Individual Cells

We next used computer simulations to test whether the observed unequal divisions, heterogeneous local growth, and slower growth of larger cells would be sufficient to reproduce the observed distribution of meristem cell sizes, assuming that the cell proliferation rate is controlled at the population level to match the rate of tissue growth (summary in Figure 2A, detailed description and source code in Supplemental Information). As a simple approximation, growth rates were adjusted to cell volume using the linear function shown in Figure 1H, but comparable results were obtained by fitting alternative functions to the data (Figures S2C–S2K) or using a probability density function (Figures S2L–S2N). Parameter values within the 95% confidence interval of experimental measurements (Table S1) were selected to minimize divergence in cell sizes (for sensitivity to parameter values, see Figures S2A and S2B). The experimental variability introduced by imaging and image processing was subtracted (Supplemental Experimental Procedures) and variation in cell-cycle length (which could not be measured at our temporal resolution) was set to zero. Even with these conservative parameter estimates, after four cell cycles the simulated cell population had significantly diverged from the tighter distribution of cell volumes seen in real meristems (Figures 2B, 2C, 2E, S2A, and S2B). In contrast, when the heterogeneity in cell growth rates was compensated by adjusting individual cell-cycle lengths (simulation *b* in Figure 2A), the simulated cell-size distribution matched the experimental data (Figures 2B, 2D, and 2E). These simulations suggested that meristem cell sizes are not stabilized as a passive consequence of the slower growth rate of larger cells, but as a result of local coordination between cell growth and cell cycle.

Meristem Cell Sizes Are Rapidly Corrected after Perturbation

Coordination of cell growth and cell cycle could occur through parallel control by external signals or by a homeostatic feedback between both processes [2]. These hypotheses make different predictions about the outcome of modifying cell sizes by transiently perturbing cell-cycle progression: parallel control would perpetuate altered cell sizes, whereas feedback would correct them [4]. To test these predictions, we used localized expression of the Kip-like CDK inhibitor KRP4, which belongs to a family of key regulators of S-phase entry in plants [17].

Previous work showed that ectopic expression of the organ growth gene *JAG* reduces meristem cell sizes by causing meristem cells to enter S-phase at abnormally small volumes [12] and that JAG directly represses *KRP4* [18]. We therefore hypothesized that *KRP4* could be an endogenous regulator of meristem cell size. Accordingly, *KRP4* was expressed in the inflorescence and floral meristems (Figures S3A–S3C), and the loss of function of *krp4-2* mutant [18] showed a small but significant reduction in meristem cell volumes (Figures S3D–S3F). Conversely, in *CLV3>>KRP4* plants, in which KRP4 was overexpressed in the

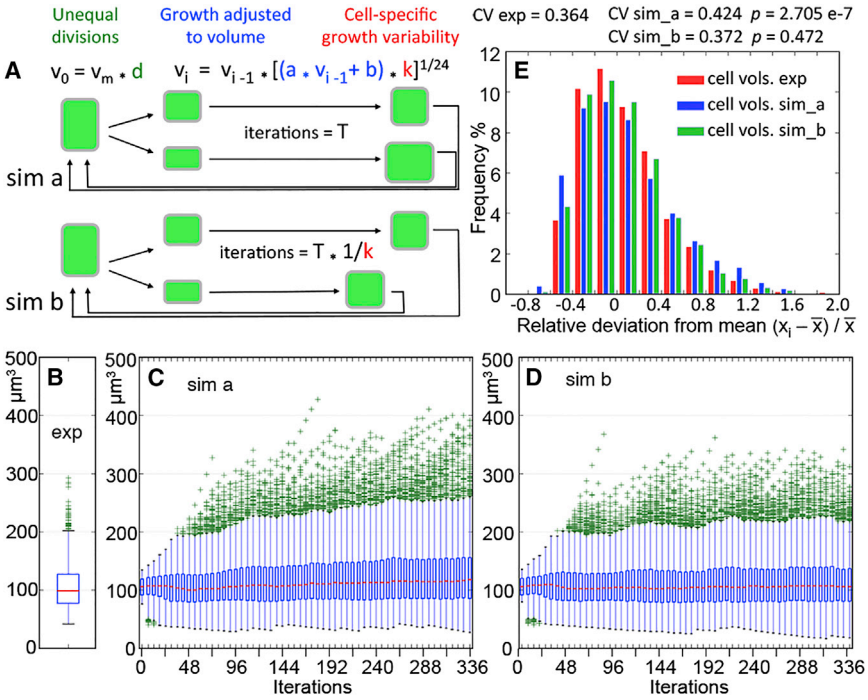

Figure 2. Comparison between Observed and Simulated Cell-Size Distributions

(A) Summary diagram of simulations; the starting cell volume v_0 results from division of the mother cell volume v_m with a variable ratio d, based on the measured SD of cell division ratios; the cell volume is updated at each iteration (equivalent to 1 hr) with the growth rate adjusted to volume by a linear function with coefficients a, b (Table S1); heterogeneous growth is introduced by a variability factor k, based on the measured LSDG (local SD of growth, defined as the SD of the relative growth rate for a cell and its neighbors); the term 1/24 is used to convert the growth rate from daily to hourly; in simulation a (sim_a), the number of growth iterations before cell division matches the average cell volume doubling time T for all cells; in sim b, the number of iterations before division was adjusted to individual cell growth rates by multiplying T by $1/k$.

(B) Boxplot of observed cell volumes in five wild-type meristems (1,746 cells).

(C and D) Boxplots of simulated volumes at different iteration numbers, using sim_a and sim_b, respectively.

(E) Frequency histograms of the deviation from the mean cell volume for sim_a and sim_b, compared with the experimental data (exp); simulation parameter values are listed in Table S1; for each set of values, data were pooled from five simulations (2,000 cells); the p values are for the hypothesis that simulated and observed cell volumes had the same coefficients of variation (CV) (Levene's test on relative deviations from mean) [13].

See also Figure S2 and Supplemental Information for simulation details and source code.

inflorescence meristem using a driver derived from the *CLV3* promoter [19], median cell volumes were nearly 4-fold higher in the center of the meristem (Figures 3A and 3D; Table S2). As the descendants of these large cells were displaced to the meristem periphery and floral primordia, where the driver was not expressed, cell volumes returned to normal, while cellular growth rates remained comparable (Figures 3G and 3H), and time-course imaging showed that cell volumes were corrected because of more frequent cell divisions (Figures 3B, 3C, 3E, 3F, and S3G–S3L). A similarly transient increase in cell sizes was seen in *CLV3>>KRP4* floral meristems (Figures S3M–S3P). We conclude that cell-cycle length is adjusted to maintain cell-size homeostasis in the meristem.

Abnormal Cell Sizes Do Not Affect Growth but Perturb Organ Boundaries and Organ Emergence

We next asked what could be the relevance of actively controlling meristem cell sizes. *CLV3>>KRP4* plants had no obvious defects in meristem size, floral bud emergence (Figures 3A and 3D), and in the overall aspect of the inflorescence (Figure S4), suggesting that as observed in leaves, meristem development can accommodate considerable variation in cell size [20]. However, because cells are the minimal spatial units to establish gene expression patterns, we reasoned that cell size might affect patterning of structures a few cells across, such as organ boundaries. To test this idea, we used an *AP1* driver [21] to overexpress KRP4 throughout floral buds (Figure 4A). Buds in equivalent positions around the apex had similar sizes in *AP1>>KRP4* and in the wild-type, suggesting that once again organ growth accommodated the increased cell size (Figures 4B and 4C). Organ boundaries, however, were wider and less well defined, both morphologically and based on the expression of a boundary marker (Figures 4B–4E and 4H–4K). Because growth is repressed at organ boundaries [23], wider boundaries due to larger cells might limit the number of cells available for primordium outgrowth. Accordingly, *AP1>>KRP4* primordia often failed to emerge (Figures 4D and 4E) and mature *AP1>>KRP4* flowers had fewer organs in the first three whorls (Figure 4L). Conversely, the *krp4-2* mutant, with smaller meristem cells, formed more sepals and petals, and fewer stamens (Figure 4L). Thus, both increased and decreased cell sizes were associated with early patterning defects in the floral buds.

DISCUSSION

Together, our data show that meristem cells actively control their size. Based on the measured sources of cell-size variation in the meristem, simulations could not reproduce the distribution of meristem cell sizes assuming that cell proliferation is controlled at the population level to match the tissue growth rate. Transient inhibition of cell-cycle progression caused increased cell sizes that were rapidly corrected after the inhibition was released. Furthermore, the changes in cell size caused by loss and gain of *KRP4* function implicated this gene in the control of meristem cell size, suggesting that as seen in budding yeast and mammalian cells [3, 9], the G1-S transition is a key control point to maintain cell-size homeostasis in the meristem.

Tight control of cell size in the meristem could seem at odds with the view that both plant and animal growth are controlled primarily at the organ level and that altered cell size can be

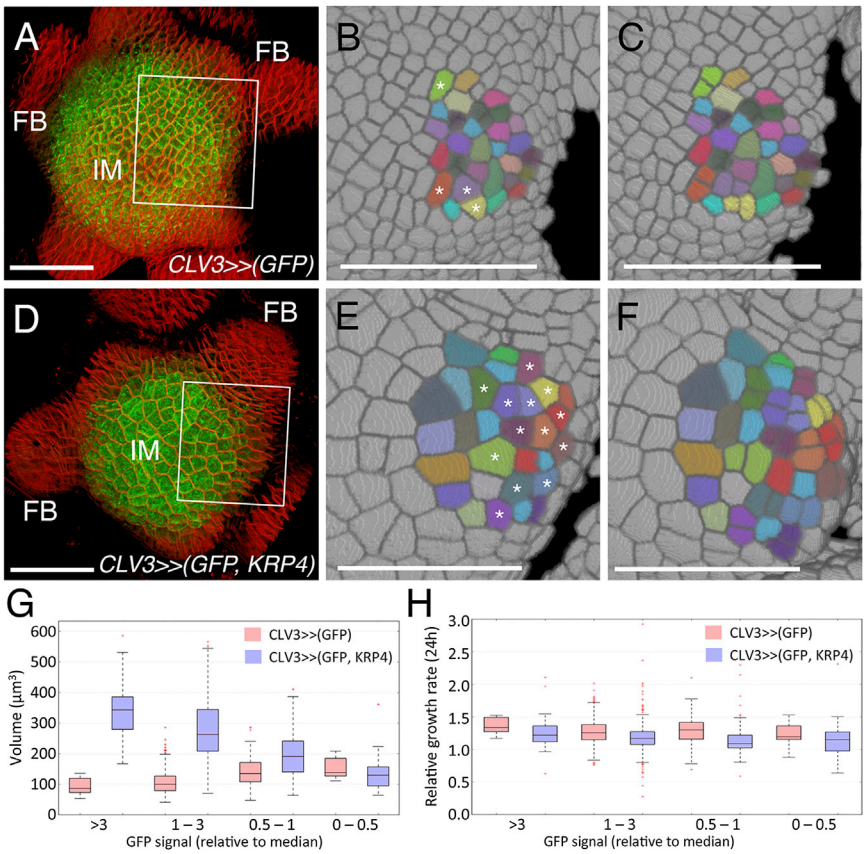

Figure 3. Recovery of Cell Volumes after Perturbation

(A and D) Confocal images of inflorescence meristems with the *CLV3:LhG4* driver directing *Op:ER-GFP* [*CLV3>>(GFP)*, A] or *Op:ER-GFP* combined with *Op:KRP4* [*CLV3>>(GFP, KRP4)*, D]; white rectangles in (A) and (D) enclose the regions corresponding to (B) and (E), respectively; note that, although the *CLV3:LhG4* driver was expressed more widely in the inflorescence meristem than the endogenous *CLV3* gene [10], it was used here only as a tool for developmentally transient expression.

(B, C, E, and F) Segmented images of emerging floral buds in *CLV3>>(GFP)* (B and C) and *CLV3>>(GFP, KRP4)* (E and F) at 0 (B and E) and 24 hr later (C and F); matching cells are in the same color and asterisks mark cells in (B) and (E) that divided after 24 hr; note in (E) and (F) the high frequency of cell divisions in cells that are being displaced from the region expressing the *CLV3:LhG4* driver.

(G and H) Boxplots of cell volumes (G) and growth rates (H) of *CLV3>>(GFP)* (red) and *CLV3>>(GFP, KRP4)* (blue) cells with different levels of GFP expression.

Scale bars, 50 μm. See also Figure S3.

compensated by changes in cell number [2, 24]. However, the compensation between cell size and cell proliferation in plants is organ specific [20], and the coordination between cell volume and cell-cycle progression changes during the transition from meristem to organ identity [12]. Based on our results, cell-size control may be especially important in the meristem and early organs because of the scale at which patterning occurs within these structures. So far, the control of cell size has been considered important primarily for cell physiology, which is affected by the volume/surface ratio [2, 24]. Our work suggests that in multicellular organisms, cell-size control can have an additional role in generating spatial detail during development.

EXPERIMENTAL PROCEDURES

Plant Material

Plants were grown on JIC *Arabidopsis* Soil Mix at 16°C under continuous light (100 μE). *Arabidopsis thaliana* accession Landsberg-*erecta* (L-*er*) was used throughout; *krp4-2*, *jag-2*, *CLV3:LhG4*, *Op:ER-GFP*, *AP1:LhG4*, and *pCUC1::CUC1-GFP* have been described [12, 19, 21, 22, 25].

For construction of *KRP4-GFP*, the *KRP4* gene (AGI: *At2g32710*) was amplified from *Arabidopsis* accession Col-0 (Chr2, nucleotides 13872160-13876781) and sGFP(S65T) [26] was inserted in frame at the end of the coding sequence before cloning into pPZP222 [27]. For creation of *Op:KRP4*, the *KRP4* coding sequence (887 bp) was PCR amplified from Col-0 cDNA, re-sequenced, and subcloned downstream of the 6XOpΩ promoter in pOWL49 [28]. Transgenic lines were generated by floral dip transformation of L-*er* plants [29]; in the case of *KRP4-GFP*, *jag-2-2 krp4-2* plants were transformed and selected for segregation as single loci and for reversion to the *jag-2* phenotype [30].

Imaging

For time-lapse imaging, inflorescence apices were prepared and imaged as described [11]. Before imaging, dissected apices were left to recover in GM medium (0.1% glucose; 0.44% Murashige and Skoog medium including vitamins, 0.9% agar [pH 5.7]) for 24 hr at 16°C, continuous light. Dissected apices were imbibed for 10 min in 50 μg/ml N-(4-triethylammoniumpropyl)-4-(p-dietheylaminophenylhexatrienyl pyridium dibromide) (FM4-64, Invitrogen) and imaged with a Zeiss LSM780 confocal microscope with excitation at 488 nm, emission filters set to 572–625 nm for FM4-64 and 505-600 nm for GFP, using a ×40/1.0 dipping objective. Image resolution was 0.42 × 0.42 × 0.5 μm.

Image Analysis

For 3D segmentation, cell measurements, matching cells at different time points and tracking cell divisions, confocal image stacks were processed using scripts written in Python 2.7.3 with functions imported from Numerical Python (http://www.numpy.org), Scientific Python (http://www.scipy.org), matplotlib (http://matplotlib.org), and SimpleITK (http://www.simpleitk.org). Fiji macros [31] were used to visualize images, select landmark points (using the 3DViewer plugin; http://fiji.sc/3D_Viewer) [32], and select cells to be removed from the analysis during manual quality control. The supplemental software file (Data S1) contains the 3D_meristem_analysis package with the annotated source code and detailed instructions on how to install and use the Python scripts and Fiji macros.

The original confocal stacks, metadata, landmark coordinates, images produced at each step of processing, and cell data tables can be found at https://open-omero.nbi.ac.uk (username "shared," password "Op3n-4cc0unt"); the folder names correspond to those listed in the raw data table (Table S2).

Statistics

For each treatment, measurements from three to five apices were pooled after filtering by cell layer, region of interest (meristem), GFP expression, and cell division, as specified in Table S2. The raw data were read and processed in a Python shell using the functions defined and annotated in script /3D_meristem_analysis/python_scripts/statistical_analysis.py (Data S1). Scipy functions were used for Pearson correlation, two-tailed Mann-Whitney tests,

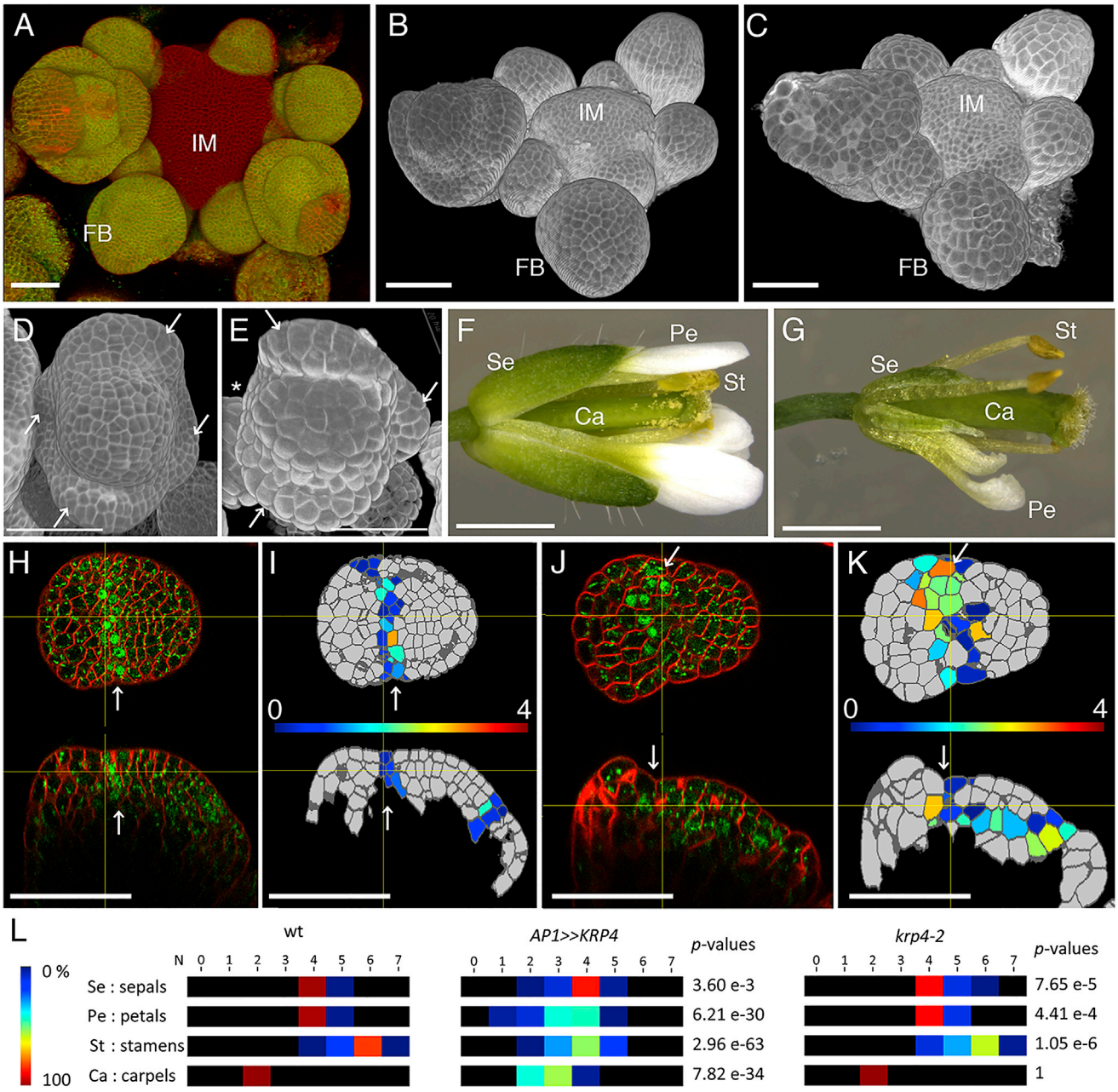

Figure 4. Abnormal Cell Sizes Affect Organ Boundaries and Primordium Emergence

(A) Expression of *AP1>>GFP* in floral buds (FB), but not in the inflorescence meristem (IM).

(B and C) Larger cells in floral buds (FB) of *AP1>>KRP4* (C) compared to the WT control (B).

(D and E) Close-up view of WT (D) and *AP1>>KRP4* (E) buds, with sepal primordia indicated by arrows; one of the lateral sepals has not emerged in E (asterisk).

(F and G) Mature flowers of WT (F) and *AP1>>KRP4* (G) with missing organs (Se, sepals; Pe, petals, St, stamens; Ca, carpels).

(H–K) Expression of the *pCUC1:CUC1-GFP* [22] organ boundary marker (arrows) in WT (H and I) and *AP1>>KRP4* (J and K), shown in confocal images (H and J) and in segmented images (I and K) with cells labeled by nuclear GFP expression; each panel shows transversal (top) and longitudinal (bottom) sections of the same bud, with horizontal lines marking the sectioning planes used.

(L) Heatmap showing the frequency of flowers with different numbers (N) of each organ type (raw data in Table S3); p values are for the equality of median organ number compared to WT (Mann-Whitney test).

Scale bars, 50 μm (A–E and H–K) and 1 mm (F and G). See also Figure S4.

least-squares fitting, and for calculating the probability density function. Confidence intervals were calculated by bootstrapping (100,000 iterations, except for linear regression, for which 10,000 iterations were used). p values for the equality of coefficients of variation were calculated by applying Levene's test on the relative deviations from the mean as described [13]. For organ counts (Table S3), plants were grown as described above until bolting; the first three flowers were discarded, and the next 15 flowers were examined from the main inflorescence of 12 individual plants of each genotype.

Simulations

Details of the simulations are given in the Supplemental Experimental Procedures and annotated source code in Data S1; parameter values are listed in Table S1.

SUPPLEMENTAL INFORMATION

Supplemental Information includes Supplemental Experimental Procedures, four figures, three tables, and one data file and can be found with this article online at http://dx.doi.org/10.1016/j.cub.2015.10.008.

AUTHOR CONTRIBUTIONS

Conceptualization, A.S.-M., K.S., and R.S.; Investigation, A.S.-M. and K.S.; Resources, K.S.; Software, Formal Analysis, and Data Curation: R.S.; Writing – Original Draft, R.S.; Writing – Review & Editing, A.S.-M., K.S., and R.S.; Funding Acquisition, R.S. and A.S.-M.; Supervision, R.S.

ACKNOWLEDGMENTS

We thank Yuval Eshed (Weizmann Institute, Israel) for the CLV3 and AP1 driver lines and Martin Howard and Richard Morris for critical comments. The work was supported by BBSRC grants BB/J007056/1 and BB/J004588/1, by a grant from the Ministerio de Educación, Cultura y Deporte, Spain (EX-2010-0491) to A.S.M., and a EU Marie-Curie fellowship (237909) to K.S.

Received: August 13, 2015
Revised: September 14, 2015
Accepted: October 5, 2015
Published: October 29, 2015

REFERENCES

1. Lloyd, A.C. (2013). The regulation of cell size. Cell *154*, 1194–1205.
2. Ginzberg, M.B., Kafri, R., and Kirschner, M. (2015). Cell biology. On being the right (cell) size. Science *348*, 1245075.
3. Turner, J.J., Ewald, J.C., and Skotheim, J.M. (2012). Cell size control in yeast. Curr. Biol. *22*, R350–R359.
4. Wood, E., and Nurse, P. (2013). Pom1 and cell size homeostasis in fission yeast. Cell Cycle *12*, 3228–3236.
5. Pan, K.Z., Saunders, T.E., Flor-Parra, I., Howard, M., and Chang, F. (2014). Cortical regulation of cell size by a sizer cdr2p. eLife *3*, e02040.
6. Killander, D., and Zetterberg, A. (1965). A quantitative cytochemical investigation of the relationship between cell mass and initiation of DNA synthesis in mouse fibroblasts in vitro. Exp. Cell Res. *40*, 12–20.
7. Dolznig, H., Grebien, F., Sauer, T., Beug, H., and Müllner, E.W. (2004). Evidence for a size-sensing mechanism in animal cells. Nat. Cell Biol. *6*, 899–905.
8. Tzur, A., Kafri, R., LeBleu, V.S., Lahav, G., and Kirschner, M.W. (2009). Cell growth and size homeostasis in proliferating animal cells. Science *325*, 167–171.
9. Kafri, R., Levy, J., Ginzberg, M.B., Oh, S., Lahav, G., and Kirschner, M.W. (2013). Dynamics extracted from fixed cells reveal feedback linking cell growth to cell cycle. Nature *494*, 480–483.
10. Aichinger, E., Kornet, N., Friedrich, T., and Laux, T. (2012). Plant stem cell niches. Annu. Rev. Plant Biol. *63*, 615–636.
11. Fernandez, R., Das, P., Mirabet, V., Moscardi, E., Traas, J., Verdeil, J.-L., Malandain, G., and Godin, C. (2010). Imaging plant growth in 4D: robust tissue reconstruction and lineaging at cell resolution. Nat. Methods *7*, 547–553.
12. Schiessl, K., Kausika, S., Southam, P., Bush, M., and Sablowski, R. (2012). *JAGGED* controls growth anisotropyand coordination between cell sizeand cell cycle during plant organogenesis. Curr. Biol. *22*, 1739–1746.
13. Van Valen, L. (2005). The statistics of variation. In Variation: A Central Concept in Biology, B. Hallgrímsson, and B.K. Hall, eds. (Academic Press), pp. 29–48.
14. Shapiro, B.E., Tobin, C., Mjolsness, E., and Meyerowitz, E.M. (2015). Analysis of cell division patterns in the Arabidopsis shoot apical meristem. Proc. Natl. Acad. Sci. USA *112*, 4815–4820.
15. Mitchison, J.M. (2003). Growth during the cell cycle. Int. Rev. Cytol. *226*, 165–258.
16. Uyttewaal, M., Burian, A., Alim, K., Landrein, B., Borowska-Wykręt, D., Dedieu, A., Peaucelle, A., Ludynia, M., Traas, J., Boudaoud, A., et al. (2012). Mechanical stress acts via katanin to amplify differences in growth rate between adjacent cells in Arabidopsis. Cell *149*, 439–451.
17. Zhao, X., Harashima, H., Dissmeyer, N., Pusch, S., Weimer, A.K., Bramsiepe, J., Bouyer, D., Rademacher, S., Nowack, M.K., Novak, B., et al. (2012). A general G1/S-phase cell-cycle control module in the flowering plant Arabidopsis thaliana. PLoS Genet. *8*, e1002847.
18. Schiessl, K., Muiño, J.M., and Sablowski, R. (2014). Arabidopsis *JAGGED* links floral organ patterning to tissue growth by repressing Kip-related cell cycle inhibitors. Proc. Natl. Acad. Sci. USA *111*, 2830–2835.
19. Goldshmidt, A., Alvarez, J.P., Bowman, J.L., and Eshed, Y. (2008). Signals derived from YABBY gene activities in organ primordia regulate growth and partitioning of Arabidopsis shoot apical meristems. Plant Cell *20*, 1217–1230.
20. Tsukaya, H. (2008). Controlling size in multicellular organs: focus on the leaf. PLoS Biol. *6*, e174.
21. Emery, J.F., Floyd, S.K., Alvarez, J., Eshed, Y., Hawker, N.P., Izhaki, A., Baum, S.F., and Bowman, J.L. (2003). Radial patterning of Arabidopsis shoots by class III HD-ZIP and KANADI genes. Curr. Biol. *13*, 1768–1774.
22. Baker, C.C., Sieber, P., Wellmer, F., and Meyerowitz, E.M. (2005). The early extra petals1 mutant uncovers a role for microRNA miR164c in regulating petal number in Arabidopsis. Curr. Biol. *15*, 303–315.
23. Rast, M.I., and Simon, R. (2008). The meristem-to-organ boundary: more than an extremity of anything. Curr. Opin. Genet. Dev. *18*, 287–294.
24. Marshall, W.F., Young, K.D., Swaffer, M., Wood, E., Nurse, P., Kimura, A., Frankel, J., Wallingford, J., Walbot, V., Qu, X., and Roeder, A.H. (2012). What determines cell size? BMC Biol. *10*, 101.
25. Ohno, C.K., Reddy, G.V., Heisler, M.G.B., and Meyerowitz, E.M. (2004). The Arabidopsis *JAGGED* gene encodes a zinc finger protein that promotes leaf tissue development. Development *131*, 1111–1122.
26. Chiu, W., Niwa, Y., Zeng, W., Hirano, T., Kobayashi, H., and Sheen, J. (1996). Engineered GFP as a vital reporter in plants. Curr. Biol. *6*, 325–330.
27. Hajdukiewicz, P., Svab, Z., and Maliga, P. (1994). The small, versatile pPZP family of Agrobacterium binary vectors for plant transformation. Plant Mol. Biol. *25*, 989–994.
28. Reddy, G.V., and Meyerowitz, E.M. (2005). Stem-cell homeostasis and growth dynamics can be uncoupled in the Arabidopsis shoot apex. Science *310*, 663–667.
29. Clough, S.J., and Bent, A.F. (1998). Floral dip: a simplified method for Agrobacterium-mediated transformation of Arabidopsis thaliana. Plant J. *16*, 735–743.
30. Schiessl, K., Muiño, J.M., and Sablowski, R. (2014). Arabidopsis *JAGGED* links floral organ patterning to tissue growth by repressing Kip-related cell cycle inhibitors. Proc. Natl. Acad. Sci. *111*, 2830–2835.
31. Schindelin, J., Arganda-Carreras, I., Frise, E., Kaynig, V., Longair, M., Pietzsch, T., Preibisch, S., Rueden, C., Saalfeld, S., Schmid, B., et al. (2012). Fiji: an open-source platform for biological-image analysis. Nat. Methods *9*, 676–682.
32. Schmid, B., Schindelin, J., Cardona, A., Longair, M., and Heisenberg, M. (2010). A high-level 3D visualization API for Java and ImageJ. BMC Bioinformatics *11*, 274.